Modified Potentials as a Tool for Computing Green's Functions in Continuum Mechanics

Yu.A. Melnikov and M.Yu. Melnikov[1]

Abstract: The use of potential (integral) representations is studied when computing Green's functions for boundary value problems stated for Laplace and biharmonic equations over regions of complex configuration in two dimensions. The emphasis is on the non-traditional potentials, whose observation and source points occupy different sets. Such potentials reduce the original boundary value problems to functional (integral) equations with smooth kernels. Special integral representations are studied, the ones whose kernels are built not of the fundamental solutions of governing differential equations but of the Green's functions for simply shaped regions, which are associated with boundary value problems under consideration. Such integral representations are called here the *modified potentials*, to the contrary of the standard potentials that are referred to as the *classical potentials*. Computability of different existing forms of Green's functions is discussed. Computational experiments have been conducted to analyze the relative effectiveness of both types of potentials when solving test problems.

1 Introduction

The idea of employing Green's functions for the formation of kernels of elliptic potential representations was introduced for the first time in the western computational mechanics-related literature in [Melnikov(1977)]. The method of modified potentials (MMP) that results from that idea, has later been employed in [Melnikov(1982), Melnikov(1995)] for solving a number of boundary value problems from various areas of computational mechanics. The MMP has been proven more effective in many cases compared to the method of classical potentials (MCP) [Brebbia(1978), Kupradze(1965), Lovitt(1950), Smirnov(1964), Tikhonov and Samarskii(1963)], which uses fundamental solutions of governing differential equations (systems) for constructing kernels of potentials.

The range of successful applications of the MMP is not that broad compared to the MCP. However, when applicable, the MMP is notably more advanced. Its superiority can be highlighted with the following two comments. First, the MMP procedures are economical computationally, because, when using this method, there is no need to numerically solve boundary integral equations over some segments of the boundary (where the boundary conditions in the original formulation are automatically satisfied by the Green's function that is constructed prior to the computational treatment). Second, it appears that Green's functions bring a big deal of stability to the numerical procedures that are used to solve the functional equations, to which the original problem is eventually reduced by the MMP.

In this study, we review computational properties of different existing forms of standard Green's functions and emphasize the importance of the compactness of those forms for numerical procedures of the MMP to be maximal effective. Computational algorithms based on this method are also analyzed by comparing them against the traditional boundary integral equation method (BIEM)-based routines. Upon considering some standard test examples for Laplace and biharmonic equation, we develop a clear understanding of strong and weak points of the MMP.

2 Computability of Green's functions

Since Green's functions are used in the MMP for constructing kernels of potentials, the compactness of a form of the Green's function becomes a defining issue, as long as the computational effectiveness of this method is considered. Indeed, only a compact, accurately computable form of the potential's kernel is efficient in practice, given the fact that the computational procedure of any version of the potential method is repeatedly recall-

---

[1] Middle Tennessee State University, Murfreesboro, Tennessee 37132 USA

ing a subroutine for computing values of the potential's kernel.

To clearly realize strengths and weaknesses of the MMP, we limit ourselves in this study to Laplace and biharmonic equation in two dimensions. Such a limitation makes sense because: (i) these equations are widely applicable in engineering and science, and (ii) there are some Green's functions for various boundary value problems, formulated for these equations, available in standard and recent texts related to mathematical physics (see, for example, [Lebedev, Skal'skaya and Uflyand(1966), Lovit(1950), Melnikov(1999), Smirnov(1964), Tikhonov and Samarskii(1963)]). Unfortunately, not all of the forms of Green's functions that are available in the literature, are appropriate for the immediate computational use.

As one of the rare examples of an immediately computable form, recall the classical [Tikhonov and Samarskii(1963)] expression

$$G_1(r,\phi;\rho,\psi) = \frac{1}{2\pi} \ln \frac{|z\overline{\zeta}-a^2|}{a|z-\zeta|} \qquad (1)$$

for the Green's function of Dirichlet problem stated for Laplace equation on the disk $\Omega_d = \{(r,\phi) : 0 < r < a,\ 0 \le \phi < 2\pi\}$. Here $z = r(\cos\phi + i\sin\phi)$ and $\zeta = \rho(\cos\phi + i\sin\phi)$ represent the observation and the source point, respectively, while $\overline{\zeta}$ stands for the complex conjugate.

In the standard Green's function-related texts (see, for example, [Lebedev, Skal'skaya and Uflyand(1966), Tikhonov and Samarskii(1963), Timoshenko and Woinowksy-Krieger(1959)]), one finds readily computable expressions for Green's functions of Dirichlet problem for such regions as a half-plane, a circular sector, an infinite strip, and a semi-strip. For example, the following expression

$$G_2(x,y;s,t) = \frac{1}{2\pi} \ln \frac{[\cosh(x+s)-\cos(y-t)][\cosh(x-s)-\cos(y+t)]}{[\cosh(x-s)-\cos(y-t)][\cosh(x+s)-\cos(y+t)]} \qquad (2)$$

represents the Green's function of Dirichlet problem for Laplace equation on the semi-strip $\Omega_{ss} = \{(x,y) : 0 < x < \infty,\ 0 < y < \pi\}$. Here (x,y) and (s,t) represent the observation and the source point, respectively.

The following classical [Lebedev, Skal'skaya and Ufly-

and(1966)] form

$$G_3(z,\zeta) =$$
$$\frac{1}{8\pi}\left[\frac{1}{2a^2}\left(a^2-|z|^2\right)\left(a^2-|\zeta|^2\right) - |z-\zeta|^2 \ln\frac{|a^2-z\overline{\zeta}|}{a|z-\zeta|}\right] \qquad (3)$$

of the Green's function for the Dirichlet-type boundary value problem

$$u(a,\phi) = 0, \quad \frac{\partial u(a,\phi)}{\partial r} = 0$$

for the biharmonic equation, formulated on the disk $\Omega_d = \{(r,\phi) : 0 < r < a,\ 0 \le \phi < 2\pi\}$ is also directly computable. In structural mechanics, the function in eqn (3) is referred to as the influence function of a unit transverse point force for a thin circular Poisson-Kirchhoff plate whose edge is built in.

Clearly, forms of the type in eqns (1)-(3) are suitable for an immediate computation, because they are expressed in terms of elementary functions. Unfortunately, only a limited number of such forms of Green's functions is available in the standard texts.

Many of the existing representations of Green's functions cannot be accurately computed. They usually require certain adjustments prior to the actual involvement in a numerical computation. Those adjustments are sometimes quite nontrivial. Recall, for example, the well-known double-Fourier series form

$$G_4(x,y;s,t) = \frac{4ab}{\pi^2}\sum_{m,l=1}^{\infty}\frac{\sin(\mu x)\sin(\mu s)\sin(\lambda y)\sin(\lambda t)}{(la)^2+(mb)^2} \qquad (4)$$

of the Green's function for Dirichlet problem stated for Laplace equation on the rectangle $\Omega_r = \{(x,y) : 0 < x < a,\ 0 < y < b\}$, where $\mu = m\pi/a$ and $\lambda = l\pi/b$. This expression is not appropriate for accurate computation, because the series in eqn (4) does not uniformly converge.

In fact, any series expansion of a Green's function for the two-dimensional Laplace equation ought to be non-uniformly convergent because of its logarithmically singular component. This computational deficiency can, however, be fixed for series representations of the type in eqn (4). From [Melnikov(1999)], for example, one learns how to reduce such series representations to accurately computable forms by the explicit split off the logarithmic singularity. Such an operation eventually yields

a uniformly convergent series for the regular component of a Green's function.

Notice that another form of $G_4(x,y;s,t)$ (alternative to that of eqn (4)) that is written [Smirnov(1964)] with the aid of the so-called Weierstrass functions, is not appropriate for computations either, because standard procedures for computing Weierstrass functions are yet unaccessible in existing software and the known expressions of these functions in terms of infinite products are cumbersome and difficult to accurately compute.

Another example of a Green's function that is not directly suitable for computing is associated with the mixed boundary value problem

$$\frac{\partial u(a,\varphi)}{\partial r} + \beta u(a,\varphi) = 0$$

stated for Laplace equation on the disk Ω_d of radius a. This Green's function

$$G_5(z,\zeta) =$$
$$\frac{1}{2\pi}\left\{\frac{1}{\beta} + \ln\frac{|z\overline{\zeta}-1|}{|z-\zeta|} + 2\Re\left[\omega^{-\beta}\int_0^\omega \frac{t^{\beta-1}}{1-t}dt\right]\right\} \qquad (5)$$

as written for the unit disk, can be found, for example, in [10]. Here $\Re$ denotes the real part of a function of complex variable, $\omega = r\rho\exp(i(\varphi-\psi))$, with (r,φ) and (ρ,ψ) representing the field and the source point, respectively.

One can readily realize that, if β is taken to infinity in the above mixed boundary condition, then the latter transforms into the Dirichlet condition. On the other hand, if β is taken to infinity, then the first and the last term in eqn (5) vanish and $G_5(z,\zeta)$ reduces to the Green's function $G_1(z,\zeta)$ of Dirichlet problem for the unit disk (see eqn (1)).

As it follows from eqn (5), the regular component of $G_5(z,\zeta)$ is expressed in terms of the real part of a complex-valued function. Hence, its accurate computing represents quite a cumbersome problem itself. This makes the entire expression in eqn (5) difficult to accurately compute.

A number of computationally sounding forms of Green's functions can be found in [Melnikov(1999)]. A variety of elliptic boundary value problems of applied mechanics are considered there. Among of those, an alternative for

eqn (5) form of $G_5(z,\zeta)$ is presented there as

$$G_5(z,\zeta) = \frac{1}{2\pi}\left[\frac{1}{a\beta} + \ln\frac{a^3}{|z-\zeta||z\overline{\zeta}-a^2|}\right.$$
$$\left. - \sum_{m=1}^\infty \frac{2a\beta}{m(m+a\beta)}\left(\frac{r\rho}{a^2}\right)^m\cos(m(\phi-\psi))\right] \qquad (6)$$

It can be readily shown that, analogously to the form of $G_5(z,\zeta)$ exhibited in eqn (5), the above expression also reduces to $G_1(z,\zeta)$, if β approaches infinity. Indeed, the series term in eqn (6) can be decomposed onto two parts as

$$\sum_{m=1}^\infty \frac{2a\beta}{m(m+a\beta)}\left(\frac{r\rho}{a^2}\right)^m\cos(m(\varphi-\psi))$$

$$= 2\sum_{m=1}^\infty \left(\frac{1}{m} - \frac{1}{m+a\beta}\right)\left(\frac{r\rho}{a^2}\right)^m\cos(m(\varphi-\psi))$$

$$= 2\sum_{m=1}^\infty \frac{1}{m}\left(\frac{r\rho}{a^2}\right)^m\cos(m(\varphi-\psi))$$

$$- 2\sum_{m=1}^\infty \frac{1}{m+a\beta}\left(\frac{r\rho}{a^2}\right)^m\cos(m(\varphi-\psi))$$

While the first of the above two series sums up [Gradstein and Ryzhik(1980), Melnikov(1995), Melnikov(1999)] as

$$2\sum_{m=1}^\infty \frac{1}{m}\left(\frac{r\rho}{a^2}\right)^m\cos(m(\varphi-\psi)) = -2\ln\frac{|z\overline{\zeta}-a^2|}{a^2},$$

the second of them vanishes, as $\beta\to\infty$. With this, one arrives at

$$\lim_{\beta\to\infty}\left(\sum_{m=1}^\infty \frac{2a\beta}{m(m+a\beta)}\left(\frac{r\rho}{a^2}\right)^m\cos(m(\varphi-\psi))\right) =$$
$$- 2\ln\frac{|z\overline{\zeta}-a^2|}{a^2}$$

Thus, the expression of $G_1(z,\zeta)$ shown in eqn (1) can be obtained as a limit of $G_5(z,\zeta)$ from eqn (6) when β is taken to infinity.

Since the regular component of the version of $G_5(z,\zeta)$ from eqn (6) is written as a uniformly convergent trigonometric series (it is readily seen that its convergence rate is of the order of $1/m^2$), this version is much more effective computationally compared to that shown in eqn (5).

Indeed, to attain a required level of accuracy when computing the expression in eqn (6), one just appropriately truncates the series.

The following compact form

$$G_6(z,\zeta) = \frac{1}{8\pi} \left\{ |z-\zeta|^2 \ln\frac{|z-\zeta|}{a} - \frac{|a^2-z\overline{\zeta}|^2}{a^2} \ln\frac{|a^2-z\overline{\zeta}|}{a^2} \right.$$
$$+ \frac{(a^2-\rho^2)(a^2-r^2)}{2a^2} \left[\frac{1+\omega}{\omega} \right.$$
$$\left. \left. -2\omega \sum_{m=1}^{\infty} \frac{1}{m(m+\omega)} \left(\frac{r\rho}{a^2}\right)^m \cos(m(\phi-\psi)) \right] \right\} \quad (7)$$

of the Green's function for the boundary value problem

$$u(a,\phi) = 0, \qquad \left(\frac{\partial^2}{\partial r^2} + \frac{\sigma}{a} \frac{\partial}{\partial r} \right) u(a,\phi) = 0$$

formulated for the biharmonic equation on a circle of radius a was also obtained in [Melnikov(1999)]. In mechanical terms, the above formulation describes the bending of a thin simply supported circular Poisson-Kirchhoff plate, and $G_6(z,\zeta)$ is referred to as the influence function of a unit transverse point force for such a plate. The parameter ω in eqn (7) is expressed in terms of the Poisson ratio σ of the material, of which the plate is made, as $\omega = (1+\sigma)/2$.

An immediate computational use of the representation in eqn (7) is promising because: (i) the "singular" component of $G_6(z,\zeta)$ is explicitly expressed in terms of elementary functions (see the first logarithmic term of eqn (7)) and (ii) the regular component of $G_6(z,\zeta)$ consists of elementary functions and a rapidly convergent trigonometric series whose convergence rate is of the order of $1/m^2$. This allows accurate numerical evaluation of the Green's function by a direct truncation of the series in eqn (7).

Clearly, for numerical procedures of the MMP to be as effective as possible, it is crucial to use the most compact and computationally sounding of all of the available forms of the required Green's function.

In the following section, we explore various options for computing Green's functions of boundary value problems for the equation of potential stated over regions of complex configuration.

3   Potential Problems

Let $G(z,\zeta)$, with z and ζ being the observation and the source point, respectively, represent the Green's function to the Dirichlet problem

$$u(z) = 0, \quad z \in \Lambda \quad (8)$$

stated for the Laplace equation

$$\Delta u(z) = 0, \quad z \in \Omega \quad (9)$$

over a simply-connected region Ω bounded with a smooth contour $\Lambda \subset C^{(1)}$. For the purpose of computing, we decompose $G(z,\zeta)$ onto the logarithmic singular and the regular harmonic $g(z,\zeta)$ component as

$$G(z,\zeta) = \frac{1}{2\pi} \ln\frac{1}{|z-\zeta|} + g(z,\zeta).$$

Since $G(z,\zeta)$ vanishes on Λ by definition, its regular component $g(z,\zeta)$, being considered as a function of z, has to be the solution to the problem

$$\Delta g(z,\zeta^*) = 0, \quad z \in \Omega \quad (10)$$

$$g(z,\zeta^*) = -T(z,\zeta^*), \quad z \in \Lambda \quad (11)$$

where ζ^* is an arbitrarily fixed point on Ω, while $T(z,\zeta^*)$ represents the trace of the singular logarithmic component of $G(z,\zeta^*)$ on Λ, that is

$$T(z,\zeta^*) = \lim_{z\to\Lambda} \left(\frac{1}{2\pi} \ln\frac{1}{|z-\zeta^*|} \right)$$

In Sections 3.1 and 3.2, we analyze various algorithms based on the potential methods for computing regular components of Green's functions.

3.1   Double-layer potential approach

In compliance with the standard (see, for instance, [Lovitt(1950), Smirnov(1964), Tikhonov and Samarskii(1963)]) MCP or BIEM routine, the solution to the problem posed with eqns (10) and (11) can be written in a form of the double-layer potential

$$g(z,\zeta^*) = \int_\Lambda \frac{\partial}{\partial\nu} \left(\ln\frac{1}{|z-t|} \right) q(t)d_t\Lambda, \quad z\in\Omega, t\in\Lambda \quad (12)$$

where ν is a normal direction to Λ at point $t \in \Lambda$. The density $q(t)$ of the above potential can be determined while satisfying the boundary condition of eqn (11). In doing so and taking into account the jump-property [5] of the double-layer logarithmic potential, one arrives at the following Fredholm integral equation of the second kind

$$-\pi q(z) + \int_\Lambda \frac{\partial}{\partial \nu}\left(\ln\frac{1}{|z-t|}\right)q(t)\,d_t\Lambda = -T(z,\zeta^*), \quad z \in \Lambda \quad (13)$$

in $q(t)$. Since the kernel of the above integral equation is a continuous function [Lovitt(1950), Smirnov(1964), Tikhonov and Samarskii(1963)], its numerical solution is quite trivial. When $q(t)$ is found and substituted into the potential of eqn (12), the latter presents an explicit expression suitable for the immediate computing of values of $g(z,\zeta^*)$ and, consequently, of $G(z,\zeta^*)$ at any point z in Ω.

Thus, the double-layer potential version of the MCP seemingly provides a solid well-posed procedure for computing Green's functions. Indeed, in the course of this method, the original two-dimensional boundary value problem in eqns (10) and (11) reduces to a regular one-dimensional integral equation, whose numerical solution is not expected to be a problem at all. However, as it sometimes happens in applied mathematics, the practical computation comes to a conflict with the theoretical expectation, revealing in our case a notable shortcoming in the method. In what follows, the shadow side of the MCP procedure is demonstrated and an alternative resolution is proposed.

To make a clear point, we have considered an elementary test example, in which the regular component

$$g(z,\zeta) = \frac{1}{2\pi}\ln\frac{|z\overline{\zeta}-a^2|}{a}$$

of the Green's function $G_1(z,\zeta)$ for a disk (see eqn (1)) has been computed with the aid of the double-layer potential version of the MCP that has just been described. The approximate solution of integral equation (13) was computed by reducing it to a system of linear algebraic equations with the quadrature formulas method (the trapezoidal rule with various number k of uniform partitioning of Λ has been used).

Table 1 exhibits some results of this numerical experiment for a unit $(a = 1)$ disk, with the source point $\zeta = (\rho, \psi)$ being fixed at $\rho = .3$ and $\psi = 0$. The values

of $G_1(z,\zeta)$ have been computed at several observation (field) points that are located on the radius $\varphi = 0$ of the disk.

From the exhibited data, it is evident that the accuracy level of the computed values of $G_1(z,\zeta)$ varies within the region. If the field point is far away from the disk's boundary (see the upper four rows in the Table), then the results are accurate enough (even for such a small partitioning number as $k = 10$). However, for any value of k, there exists the near-boundary zone within which the computed values of $G_1(z,\zeta)$ notably diverge from the exact ones. Although the zone shrinks for greater k's, it still remains relatively large $(r > .9)$, even for $k = 200$, the level that is pretty close to the reasonable limit for contemporary PC's (requiring several minutes for the resulting system of linear algebraic equations to be solved).

The recorded effect of accuracy loss in computing values of the double-layer potential when the observation point approaches the region's boundary (it is referred to as the *near-boundary phenomenon*) is not directly associated with the low accuracy level of the trapezoidal rule that was actually used for numerical solution of the integral equation in (13). However, the near-boundary phenomenon can certainly be leveled to a reasonable extend with switching to some specialized quadrature formulae.

The use of more safisticated quadrature formulae (Chebyshev or even Gauss formulas, for example) can somewhat improve the situation. Of course, a more accurate method requires smaller number of partitioning points to attain the required level of accuracy. And this is, perhaps, what is usually expected when one switches from a less accurate quadrature method to a more advanced one. However, computational algorithms for more accurate methods are usually more time consuming. And this could nullify the computational superiority of a more accurate method.

It appears that the actual cause for the near-boundary phenomenon is directly related to the jump-property of the double-layer potential. Since the latter is discontinuous when the observation point crosses the region's boundary, we can say that this phenomenon resembles the classical Gibbs phenomenon that occurs when a discontinuous function is approximated with a continuous one at the vicinity of a point of discontinuity. Hence, the accuracy loss occurs not when eqn (12) is solved but rather when the potential in eqn (13) is computed. As a result, the near-boundary phenomenon is hard to com-

Table 1 : Values of $G_1(z,\zeta)$ computed by the double-layer potential

Field	Partitioning number, k					Exact
point, r	10	20	50	100	200	values
.00	.191618	.191618	.191618	.191618	.191618	.191618
.20	.356589	.356620	.356620	.356620	.356620	.356620
.40	.346163	.346122	.346122	.346122	.346122	.346122
.60	.159207	.160029	.160033	.160034	.160034	.160034
.80	.052434	.065258	.066637	.066639	.066640	.066640
.90	-.030148	.015349	.030619	.031210	.031211	.031213
.95	-.154620	-.048418	.005684	.014491	.015017	.015169
.99	-1.07095	-.507030	-.170941	-.062585	-.014595	.002971

pletely avoid within the scope of the double-layer potential version of the MCP.

3.2 Single-layer-type potential approach

Thus, from the previous section, it follows that the double-layer potential approach in its classical version is not a reasonable technique for the uniformly accurate computing of Green's functions. In looking for the alternative method that would be free from the near-boundary phenomenon and would, consequently, allow accurate computing throughout the entire region, we come up with an alternative potential approach rooted in the method of functional equations [Kupradze(1965)]. That is, to compute the regular component $g(z,\zeta^*)$ of a Green's function, the single-layer-type logarithmic potential

$$g(z,\zeta^*) = \int_{\Lambda_0} \ln\frac{1}{|z-t|} q(t)d_t\Lambda_0, \quad z\in\Omega,\, t\in\Lambda_0 \qquad (14)$$

is suggested for the solution of the boundary value problem posed with eqns (10) and (11). The contour Λ_0 (referred to as the *ficticioius* contour) in eqn (14) is a closed curve that embodies the actual contour Λ of Ω. Clearly, $g(z,\zeta^*)$ given by eqn (14), is a harmonic function of z in Ω. Since potential (14) is continuous, when the field point approaches and crosses the actual region's contour Λ, the following functional equation

$$\int_{\Lambda_0} \ln\frac{1}{|z-t|} q(t)d_t\Lambda_0 = -T(z,\zeta^*), \quad z\in\Lambda,\, t\in\Lambda_0 \qquad (15)$$

appears while satisfying the boundary condition of eqn (11).

Due to the fact that the kernel of potential (14) is the fundamental solution of Laplace equation, we call this approach the single-layer-type potential version of the MCP.

To make the described approach practical, certain recommendations ought to be worked out as to the shape and location of Λ_0. From our experience, it follows that, for a wide range of shapes of Ω, the best regularizing effect is attained when Λ_0 is taken as just a circle whose radius is of the order of .6 to 1.0 times the biggest diameter of Ω, with the distance from Λ_0 to the closest point of the actual contour Λ being greater than at least .05 to .10 times the biggest diameter of Ω.

Analogously to the procedure that was used for eqn (13) in the double-layer potential approach, we have used here the trapezoidal rule (with k uniform subdivisions of Λ and Λ_0) to obtain the numerical solution of eqn (15). To demonstrate the accuracy level of this approach, the values of $G_1(z,\zeta)$ for a unit disk have again been computed at the same set of field points as earlier. The results of this experiment are exhibited in Table 2.

Two essential observations follow from the data of Table 2. First, no near-boundary phenomenon has been recorded at all in the single-layer-type potential version of the MCP and the accuracy level attained here, on the contrary to the results shown in Table 1, is uniform for the entire region. Second, this approach is more accurate overall. Indeed, even with $k=10$ the maximum relative error of computing does not exceed the level of .01%. It is also important to note that, since in the course of the single-layer-type potential approach, the original problem reduces to a one-dimensional functional (integral) equation, the complexity of the shape of the given region could not be a decisive issue for this computational procedure. In other words, the required computer time and the accuracy level of the output are not expected to significantly vary with the shape of Ω. In Figure 1, one

Table 2 : Values of $G_1(z,\zeta)$ obtained by the single-layer-type potential

Field	Partitioning number, k					Exact
point, r	10	20	50	100	200	values
.00	.191618	.191618	.191618	.191618	.191618	.191618
.20	.356626	.356620	.356620	.356620	.356620	.356620
.40	.346140	.346123	.346122	.346122	.346122	.346122
.60	.160067	.160034	.160034	.160034	.160034	.160034
.80	.066685	.066643	.066640	.066640	.066640	.066640
.90	.031249	.031213	.031213	.031213	.031213	.031213
.95	.015193	.015170	.015169	.015169	.015169	.015169
.99	.002977	.002972	.002971	.002971	.002971	.002971
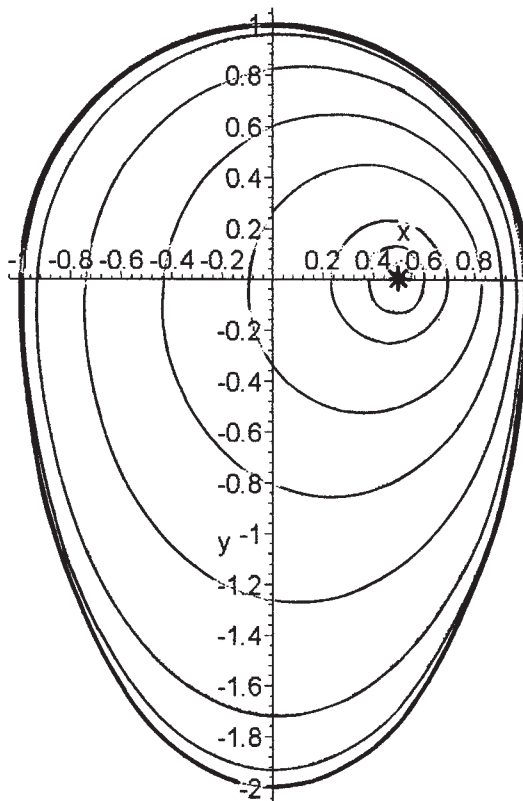
Figure 1 : Green's function for the egg-shaped region

finds, for example, the profile of the Green's function of Dirichlet problem for the egg-shaped region whose upper xy-half-plane portion represents a unit half-disk, while its lower xy-half-plane portion is a half-ellipse with 1.0 and 2.0 being the x and y semi-axes, respectively. The source point is fixed at $(.5,.0)$. Eqn (19) was solved by using the trapezoidal rule with $k = 30$. The fictitious contour Λ_0 was fixed as a circle of radius 2.5 centered at the origin.

The single-layer-type potential approach appears to be computationally effective not only when computing Green's functions for Dirichlet problem. Consider, for example, the mixed condition

$$\frac{\partial u(z)}{\partial n} + \beta u(z) = 0, \quad z \in \Lambda, \ \beta > 0 \tag{16}$$

imposed on the boundary Λ of the simply-connected region Ω. Here n represents the normal direction to Λ at z. Clearly, for an arbitrarily fixed source point ζ^*, the regular component $g(z,\zeta^*)$ of the Green's function for the problem posed with eqns (9) and (16) has to be the solution to the problem

$$\Delta g(z,\zeta^*) = 0, \quad z \in \Omega \tag{17}$$

$$\left(\frac{\partial}{\partial n} + \beta\right) g(z,\zeta^*) = -T_n(z,\zeta^*), \quad z \in \Lambda \tag{18}$$

where $T_n(z,\zeta^*)$ is defined as

$$T_n(z,\zeta^*) = \lim_{z \to \Lambda} \left(\frac{\partial}{\partial n} + \beta\right) \left(\frac{1}{2\pi} \ln \frac{1}{|z - \zeta^*|}\right)$$

Apparently, potential (14) can also be used to solve the problem in eqns (17) and (18). To find the density $q(t)$ of

(14), one arrives in this case at the following functional equation

$$\int_{\Lambda_0} \left(\frac{\partial}{\partial n} + \beta \right) \ln \frac{1}{|z-t|} \, q(t) d_t \Lambda_0 = -T_n(z,\zeta^*), z \in \Lambda, t \in \Lambda_0 \quad (19)$$

When the approximate solution of the above equation is obtained, the computed values of $q(t)$ can be used in the potential of eqn (14) to obtain values of $g(z,\zeta^*)$ and than of $G(z,\zeta^*)$ at any point z in Ω.

Table 3 : Values of $G_5(z,\zeta)$ obtained by the single-layer-type potential

Field	Partitioning number, k			Exact
point, x	10	20	50	values
-1.0	.099230	.098974	.098972	.098972
-0.8	.120686	.120397	.120396	.120396
-0.6	.146119	.145812	.145810	.145810
-0.4	.177136	.176806	.176804	.176804
-0.2	.216519	.216163	.216162	.216162
0.0	.269860	.269473	.269473	.269473
0.2	.351493	.351069	.351067	.351067
0.4	.527423	.526944	.526942	.562942
0.6	.529542	.528992	.528990	.528990
0.8	.358294	.357667	.357665	.357665
1.0	.282741	.282118	.282116	.282116

As a validation example, we have computed the Green's function $G_5(z,\zeta)$ (see eqn (6)) of the mixed boundary value problem posed with eqns (9) and (16) for a unit disk. Numerical solution of eqn (19) has been obtained with the aid of the trapezoidal rule. Table 3 illustrates the accuracy level attained in this case. The parameter β in the boundary condition of eqn (18) was chosen as $\beta = 1$, and the source point ζ was fixed at $\zeta^* = (.5, .0)$. The approximate values of $G_5(z,\zeta^*)$ has been computed for a set of field points uniformly spaced on the horizontal diameter $(-1 \le x \le 1)$ of the disk. Highly accurate results have been obtained, when Λ_0 was fixed as a circle of radius 2.0 concentric with the actual boundary Λ of the disk.

From the data of Table 3, it is evident that the method converges at a very high rate. Indeed, even with $k = 10$ the maximum relative error of the computed data stays at the level of about .1% (which itself is high enough for most possible applications), while with $k = 20$ it drops down to an impressive level of .0005%.

Note that the effective use of the single–layer-type potential version of the MCP is not limited to simply-connected regions. To illustrate the point, we consider the doubly connected region Ω whose outer contour Λ represents a piecewise smooth line $(\Lambda \subset C)$ that may contain the point at infinity, while its inner contour Γ is a smooth closed line $(\Gamma \subset C^{(1)})$. In looking for the Green's function $G(z,\zeta)$ of Dirichlet problem stated over Ω, we split off its singular component in the standard manner and then arrive, consequently, at the following boundary value problem

$$\Delta g(z,\zeta) = 0, \quad z \in \Omega \quad (20)$$

$$g(z,\zeta) = -T_\Lambda(z,\zeta), \quad z \in \Lambda \quad (21)$$

$$g(z,\zeta) = -T_\Gamma(z,\zeta), \quad z \in \Gamma \quad (22)$$

for the regular component $g(z,\zeta)$ of $G(z,\zeta)$. Here $T_\Lambda(z,\zeta)$ and $T_\Gamma(z,\zeta)$ represent the traces of the singular component of $G(z,\zeta)$ on Λ and Γ, respectively. That is,

$$T_\Lambda(z,\zeta) = \lim_{z \to \Lambda} \left(\frac{1}{2\pi} \ln \frac{1}{|z-\zeta|} \right)$$

and

$$T_\Gamma(z,\zeta) = \lim_{z \to \Gamma} \left(\frac{1}{2\pi} \ln \frac{1}{|z-\zeta|} \right).$$

The solution to the problem that appears in eqns (20)-(22), can be found as the sum of the logarithmic potentials

$$\begin{aligned} g(z,\zeta) &= \int_{\Lambda_0} \ln \frac{1}{|z-t|} q_e(t) d_t \Lambda_0 \\ &+ \int_{\Gamma_0} \ln \frac{1}{|z-t|} q_i(t) d_t \Gamma_0, \quad z \in \Omega \end{aligned} \quad (23)$$

where Λ_0 represents a closed line that embodies Λ, while Γ_0 is a closed line embodied with Γ. The densities $q_e(t)$ and $q_i(t)$ of the above potentials can be determined when satisfying the boundary conditions imposed with eqns (21) and (22). In doing so, one arrives at the functional (integral) equation

$$\begin{aligned} &\int_{\Lambda_0} \ln \frac{1}{|z-t|} q_e(t) d_t \Lambda_0 \\ &+ \int_{\Gamma_0} \ln \frac{1}{|z-t|} q_i(t) d_t \Gamma_0 = -T_\Lambda(z,\zeta), \; z \in \Lambda \end{aligned} \quad (24)$$

when satisfying the condition in eqn (21) (as z is taken to the actual outer contour Λ), while the other functional equation

$$
\int_{\Lambda_0} \ln \frac{1}{|z-t|} q_e(t) dt \Lambda_0
$$
$$
+ \int_{\Gamma_0} \ln \frac{1}{|z-t|} q_i(t) dt \Gamma_0 = -T_\Gamma(z,\zeta), \quad z \in \Gamma \qquad (25)
$$

results from taking z to the actual inner contour Γ. The system of eqns (24) and (25) can readily be solved by means of the quadrature formulas method (the trapezoid rule with uniform partitioning of both Λ_0 and Γ_0 has been used to compute the data for the illustrative examples that follow).

When the densities $q_e(t)$ and $q_i(t)$ are found and their values are substituted into (23), the latter presents an explicit expression suitable for the immediate computing values of $g(z,\zeta)$ and, consequently, of $G(z,\zeta)$ at any point in Ω.

As an illustrative example, we consider the doubly connected region whose outer contour is a unit circle, while the inner one is a circle defined as

$$
x = x_0 + a\cos(\varphi); \quad y = a\sin(\varphi)
$$

Figure 2 depicts the Green's function of Dirichlet problem for this region, with the aperture's parameters chosen as $a = .4$, and $x_0 = -.4$. The source point is fixed at $(.0, .75)$. The fictitious contours Γ_0 and Λ_0 were in this case fixed as circles of radii .2 and 2.0, centered at $(-.4, .0)$ and at the origin, respectively. Some information regarding the accuracy level attained in this case, is available in the next section (see Table 4), where we compare the effectiveness of the two alternative potential approaches.

Clearly, the procedure that was just described, is suitable for any other well-posed problem stated for a doubly connected region, with the traces $T_\Lambda(z,\zeta)$ and $T_\Gamma(z,\zeta)$ being accordingly precomputed on the outer and inner boundaries of the region. The procedure can also be extended to multi-connected regions.

3.3 The MMP approach

In many situations, especially when dealing with multi-connected regions, an alternative to the MCP approach can be suggested for computing Green's functions, the
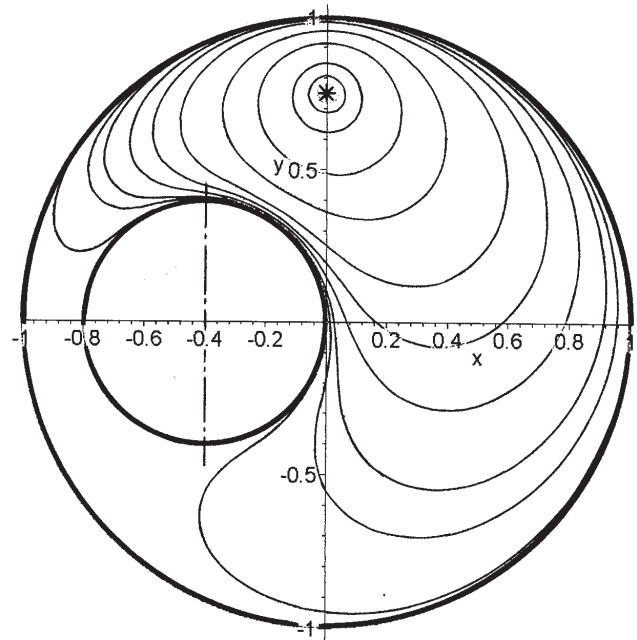
Figure 2 : Green's function for the eccentric ring

one that quite often appears to be much less computationally expensive compared to the MCP. To introduce the chief idea of the alternative approach, let us turn back to the problem of finding the Green's function $G(z,\zeta)$ of Dirichlet problem posed over the doubly connected region Ω whose outer contour is $\Lambda \subset C$ while its inner contour $\Gamma \subset C^{(1)}$.

Let $G_0(z,\zeta)$ represent the Green's function of Dirichlet problem posed over the simply-connected region Ω^* bounded by Λ. As was suggested in [Melnikov(1995)], we split off the singular component of $G(z,\zeta)$ in a manner which is different of that proposed earlier in Section 3. Namely, we decompose $G(z,\zeta)$ onto the regular $g(z,\zeta)$ and singular parts as

$$
G(z,\zeta) = G_0(z,\zeta) + g(z,\zeta).
$$

With this, $g(z,\zeta^*)$, as a function of z, must be harmonic in Ω for any arbitrarily fixed position ζ^* of the source point, and, since $G_0(z,\zeta^*)$ vanishes on Λ, $g(z,\zeta^*)$ has to satisfy the boundary conditions

$$
g(z,\zeta^*) = 0, \quad z \in \Lambda \qquad (26)
$$

$$
g(z,\zeta^*) = -G_0(z,\zeta^*), \quad z \in \Gamma \qquad (27)
$$

The solution to the problem given by (20), (26), and (27) can be written in a form of a modified single–layer–type potential whose kernel is not the fundamental solution of Laplace equation but is instead $G_0(z, \zeta)$. That is

$$g(z, \zeta^*) = \int_{\Gamma_0} G_0(z, t) q(t) d_t \Gamma_0, \quad z \in \Omega \tag{28}$$

The above potential vanishes on Λ because of the defining property of $G_0(z, \zeta^*)$. That is, it automatically satisfies the boundary condition in eqn (26). The density $q(t)$ of the potential can be determined by satisfying the boundary condition of eqn (27). This yields the following functional equation

$$\int_{\Gamma_0} G_0(z, t) q(t) d_t \Gamma_0 = -G_0(z, \zeta^*), \quad z \in \Gamma \tag{29}$$

in $q(t)$. Once the solution of (29) is found, the potential in eqn (28) presents an explicit expression for $g(z, \zeta^*)$ suitable for immediate computing of values of $G(z, \zeta^*)$ at any point $z \in \Omega$.

To our best knowledge, there is not a single boundary value problem known for Laplace equation formulated over a doubly connected region, whose Green's function is suitable for an immediate computation. In view of this circumstance, we have conducted a computational experiment allowing to check out, to a certain extend, the effectiveness of the MMP procedure that was just described. We used this procedure to compute values of the Green's function for the region shown in Figure 2, and compared them against those earlier obtained by the single-layer-type MCP procedure discussed in the previous section. Table 4 contains some data that reveal weak and strong points of both approaches and show their comparative degree of productivity. The values of $G(z, \zeta^*)$ have been computed at the set of field points uniformly spaced on the segment $x = 0$, $0 \le y \le 1$, with the source point ζ^* being fixed at $(.0, .75)$.

In computing the data for Table 4, both the system of eqns (24) and (25), on one side, and eqn (29), on the other side, were solved by the trapezoidal rule with a uniform partitioning of the fictitious contours Λ_0 and Γ_0. To adequately interpret the results of the experiment, it is important to outline that the same partitioning number k yields different computational expenses for the MCP and MMP procedures, because it represents the number of elementary segments on which each line Λ_0 and Γ_0
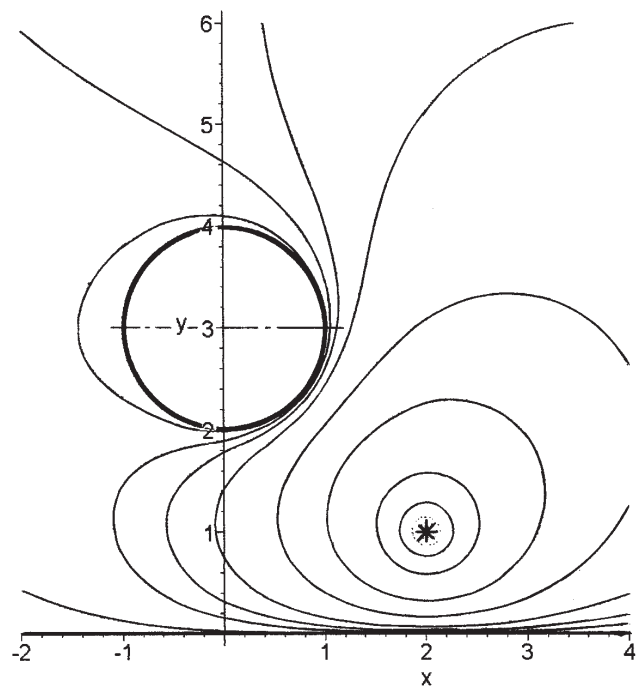
Figure 3 : Green's function for the half-plane with an apeture

is partitioned. Therefore, since both Λ_0 and Γ_0 are partitioned in the MCP procedure, whereas only Γ_0 is partitioned in the MMP procedure, the dimensions of the systems of linear algebraic equations, to which the corresponding functional equations are reduced, are $2k \times 2k$ for MCP and $k \times k$ for MMP. This, subsequently, makes the latter approach much less expensive computationally for the same value of k.

From the data of Table 4, it is evident that both the MCP and MMP procedures allow to attain a compatible degree of accuracy. However, our experience shows that MMP has proven notably more advanced, mostly because it is about eight to ten times less expensive compared to MCP. It also converges faster and more accurately satisfies the boundary conditions.

Note, in addition, that the MMP is especially effective for multi-connected regions with the outermost contour containing the point at infinity. The point is that the classical potential approaches could not be effective for unbounded regions, because they require approximate integration along the entire boundary, whereas, for the MMP, the unboundedness of a region under considera-

Table 4 : Comparison of the MCP and MMP procedures

Field point, y	MCP			MMP		
	Partitioning number, k					
	10	20	50	10	20	50
.0	-.000280	-.000128	-.000067	-.000107	.000049	-.000032
.2	.010667	.010712	.010781	.010700	.010779	.010798
.4	.062359	.062411	.062443	.062407	.062435	.062448
.6	.177534	.177574	.177585	.177583	.177590	.177593
.8	.317893	.317902	.317911	.317907	.317913	.317914
1.0	.000014	.000006	.000002	.000000	.000000	.000000

tion brings no additional complications, given that the Green's function for the corresponding simply-connected region is available.

As an illustrative example, we computed the Green's function $G(z,\zeta)$ for a half-plane $y \geq 0$ having a circular aperture Γ defined as

$$x = a\cos(t), \quad y = y_0 + a\sin(t)$$

The classical [Tikhonov and Samarskii(1963)] Green's function of Dirichlet problem for a half-plane

$$G_{hp}(z,\zeta) = \frac{1}{2\pi} \ln \frac{|z-\overline{\zeta}|}{|z-\zeta|}$$

was used as the kernel $G_0(z,\zeta)$ of the potential in eqn (28). The fictitious contour Γ_0 was selected as a circle of radius $a/2$ centered at $(0,y_0)$. Figure 3 depicts the profile of $G(z,\zeta^*)$ with the geometric parameters given as $a = 1.0$, and $y_0 = 3.0$. The source point ζ^* was put at $(2.0, 1.0)$.

Another example of a Green's function for the potential problem stated over a multi-connected region, whose outermost contour contains the point at infinity, is shown in Figure 4. To demonstrate the computational productiveness of the MMP technique, we considered the problem formulated for the semi-strip $\Omega_{ss} = \{(x,y) : 0 < x < \infty, \ 0 < y < 1\}$, having three circular apertures of radii .15, .10 and .05 centered at $(.45,.30)$, $(.30,.80)$, and $(.90,.55)$, respectively. The Dirichlet condition $u(x,y) = 0$ was imposed on the contour of each aperture. The following set of mixed boundary conditions

$$\frac{\partial u(0,y)}{\partial x} - \beta u(0,y) = u(x,0) = \frac{\partial u(x,1)}{\partial y} = 0, \quad \beta \geq 0$$
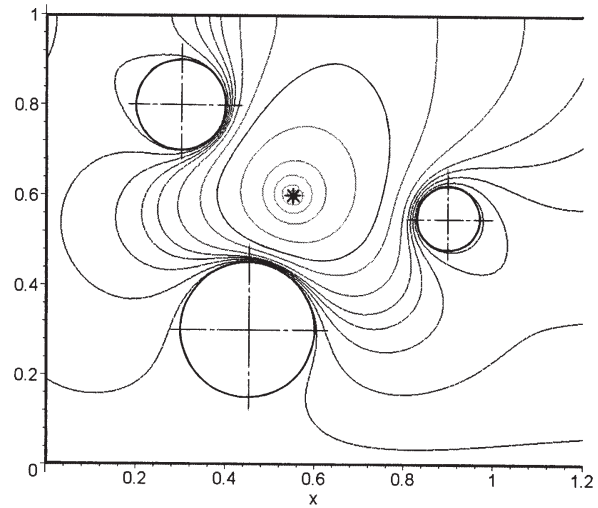
Figure 4 : Mixed problem over the multi-connected region

was assumed on the contour of Ω_{ss}. The source point has been put at $(.55, .60)$.

The parameter β in the boundary condition imposed on the segment $x = 0$ of the boundary was chosen in this case as 3.0. The fictitious contours were fixed as circles concentric with the apertures, with their radii being two times as small as the apertures' radii. Computationally effective expression of the Green's function of the above mixed boundary value problem for Laplace equation posed over the solid semi-strip Ω_{ss} is presented in [Melnikov(1999)]. It has been used in this case as the kernel $G_0(z,\zeta)$ of the potential in eqn (28).

4 Influence Functions for Poisson-Kirchhoff Plates

In this section, we extend the single-layer-type potential technique to the computing of Green's functions for equations of higher order. It will be also shown that, when the MMP is applicable, its numerical superiority against the MCP increases with the order of the governing differential equation.

The emphasis here is on boundary value problems for the biharmonic equation, the ones that simulate (within the scope of the classical Poisson-Kirchhoff theory) the bending of a thin plate having a uniform thickness and made of an isotropic homogeneous material. Let the middle surface of the plate occupy region Ω, and the plate's smooth contour Λ be clamped. The bending of such a plate can be [Timoshenko and Woinowsky-Krieger(1959)] described with the problem

$$\Delta\Delta u(z) = 0, \quad z \in \Omega \tag{30}$$

$$u(z) = 0, \quad \frac{\partial u(z)}{\partial n} = 0, \quad z \in \Lambda \tag{31}$$

where Δ is the Laplace operator and n represents the normal to Λ at z.

In Sections 4.1 and 4.2, we will develop practical algorithms based on the potential method for computing influence functions [Melnikov(1999)] of a unit transverse point force for Poisson-Kirchhoff plates. In other words, we will compute Green's functions for boundary value problems of the type in eqns (30) and (31), as well as for some other problems, for biharmonic equation.

4.1 Singe-layer-type potential procedure

Let the source point ζ in the Green's function $G(z,\zeta)$ of the problem posed with eqns (30) and (31) be fixed at an arbitrary position $\zeta^* \in \Omega$. To compute values of $G(z,\zeta^*)$, we decompose it on the singular and regular components

$$G(z,\zeta^*) = \frac{1}{8\pi}|z-\zeta^*|^2 \ln|z-\zeta^*| + g(z,\zeta^*) \tag{32}$$

Since $G(z,\zeta^*)$ satisfies, by definition, the boundary conditions imposed by eqn (31), its regular component $g(z,\zeta^*)$ has to be the solution to the problem

$$\Delta\Delta g(z,\zeta^*) = 0, \quad z \in \Omega$$

$$g(z,\zeta^*) = -\frac{1}{8\pi}|z-\zeta^*|^2 \ln|z-\zeta^*|, \quad z \in \Lambda \tag{33}$$

$$\frac{\partial}{\partial n}g(z,\zeta^*) = -\frac{1}{8\pi}\frac{\partial}{\partial n}\left(|z-\zeta^*|^2 \ln|z-\zeta^*|\right), \quad z \in \Lambda \tag{34}$$

We look for $g(z,\zeta^*)$ in a form of the biharmonic single-layer-type potential

$$g(z,\zeta^*) = \int_{\Lambda_0}\left[|z-t|^2\ln|z-t|q_1(t) + \frac{\partial}{\partial\nu}\left(|z-t|^2\ln|z-t|\right)q_2(t)\right]d_t\Lambda_0, \quad z \in \Omega \tag{35}$$

where Λ_0 represents a fictitious contour that embodies Λ and ν denotes the normal to Λ_0 at t. The densities $q_1(t)$ and $q_2(t)$ of the above potential can be determined when satisfying the boundary conditions imposed by eqns (33) and (34). In doing so, one arrives at the following system

$$\int_{\Lambda_0}\begin{pmatrix}K_{11}(z,t) & K_{12}(z,t)\\ K_{21}(z,t) & K_{22}(z,t)\end{pmatrix}\begin{pmatrix}q_1(t)\\ q_2(t)\end{pmatrix}d_t\Lambda_0 = \begin{pmatrix}f_1(z)\\ f_2(z)\end{pmatrix}, z \in \Lambda \tag{36}$$

of functional (integral) equations in $q_1(t)$ and $q_2(t)$. Here, we have

$$K_{11}(z,t) = |z-t|^2\ln|z-t|, \quad K_{12}(z,t) = \frac{\partial}{\partial\nu}K_{11}(z,t),$$

$$K_{21}(z,t) = \frac{\partial}{\partial n}K_{11}(z,t), \quad K_{22}(z,t) = \frac{\partial^2}{\partial n\partial\nu}K_{11}(z,t),$$

and

$$f_1(z) = -\frac{1}{8\pi}|z-\zeta^*|^2\ln|z-\zeta^*|, \quad f_2(z) = \frac{\partial}{\partial n}f_1(z),$$

with n being the normal to the contour Λ at point z. The system of eqn (36) can readily be solved by means of the quadrature formulas method. The trapezoidal rule with a uniform partitioning of Λ and Λ_0 has been used for the illustrative examples that follow.

After computing values of the densities $q_1(t)$ and $q_2(t)$, values of $G(z,\zeta^*)$ can be obtained with the aid of eqns (35) and (32), at any point $z \in \Omega$. This approach is extendable to other types of edge conditions imposed on Λ. In what follows, we applied it, for instance, to a circular simply supported plate.

Table 5 : $G_3(z,\zeta)$ and $G_6(z,\zeta)$ obtained by thesingle-layer-type potential

Field point,	$G_3(z,\zeta)$			$G_6(z,\zeta)$		
	Partitioning number, k					
x	10	50	exact	10	50	exact
-1.0	.0000000	.0000000	.0000000	.0000000	.0000000	.0000000
-0.8	.0007518	.0007496	.0007496	.0091152	.0091221	.0091221
-0.6	.0028599	.0028565	.0028565	.0183925	.0184045	.0184047
-0.4	.0060459	.0060438	.0060438	.0273714	.0273794	.0273796
-0.2	.0099032	.0099052	.0099052	.0354198	.0354244	.0354245
0.0	.0137838	.0137924	.0137925	.0416400	.0416446	.0416446
0.2	.0164637	.0164881	.0164882	.0445321	.0445394	.0445395
0.4	.0143165	.0143419	.0143419	.0401278	.0401307	.0401309
0.6	.0079604	.0079856	.0079857	.0286579	.0286655	.0286655
0.8	.0023396	.0023523	.0023524	.0146123	.0146194	.0146194
1.0	.0000000	.0000000	.0000000	.0000000	.0000000	.0000000

To illustrate the computational effectiveness of the approach, two validation examples have been considered for a circular plate of radius $a = 1.0$. Namely, approximate values of the influence function $G_3(z,\zeta)$ (clamped edge) and $G_6(z,\zeta)$ (simply supported edge) have been computed and compared against their exact values found with the aid of the expressions from eqns (3) and (7). The computation has been carried out for a set of field points uniformly spaced on the diameter ($-1 \le x \le 1$) of the plate. The source point ζ was fixed, in both cases, at $\zeta^* = (.3, .0)$. The results of this experiment are exposed in Table 5. The exhibited data demonstrate rather high degree of accuracy and fast convergence of the method.

Note that the influence function in the plate theory represents the deflection of a plate that is caused by a transverse unit point force. Hence, to obtain the components of the associated stress state, one is required to compute partial derivatives of the second and the third order of the influence function. In light of this, it is important to note that no numerical differentiation is required here, because any order partial derivative of the potential of eqn (35) can be taken analytically. This, therefore, allows us to compute stress components in the plate with the same accuracy level as attained for the deflection function.

4.2 The MMP procedure

The version of the MMP developed in Section 3.3, is extended here to plate problems. Consider the boundary value problem

$$B_{\lambda_1} u(z) = 0, \quad B_{\lambda_2} u(z) = 0, \quad z \in \Lambda \tag{37}$$

$$B_{\gamma_1} u(z) = 0, \quad B_{\gamma_2} u(z) = 0, \quad z \in \Gamma \tag{38}$$

stated for eqn (30) over the doubly connected region whose smooth outer and inner contours are Λ and Γ, respectively. We assume that the problem in eqns (30), (37), and (38) is well-posed (has only the trivial solution).

Suppose $G_0(z,\zeta)$ represents the Green's function of the problem posed with eqns (30) and (37) over the simply-connected region Ω^* bounded with Λ. Analogously to Section 3.3, we break down the Green's function $G(z,\zeta)$ of the problem in eqns (30), (37), and (38) onto the singular $G_0(z,\zeta)$ and the regular $g(z,\zeta)$ components as

$$G(z,\zeta) = G_0(z,\zeta) + g(z,\zeta).$$

Since $G_0(z,\zeta^*)$ satisfies the boundary conditions imposed by eqn (37) for any position ζ^* of the source point, the regular component $g(z,\zeta^*)$, as a function of z, must be the solution to the problem

$$\Delta\Delta g(z,\zeta^*) = 0, \quad z \in \Omega$$

$$B_{\lambda_1} g(z,\zeta^*) = 0, \quad B_{\lambda_2} g(z,\zeta^*) = 0, \quad z \in \Lambda \tag{39}$$

$$B_{\gamma_1} g(z,\zeta^*) = T_{\gamma_1}(z), \quad B_{\gamma_2} g(z,\zeta^*) = T_{\gamma_2}(z), \quad z \in \Lambda \quad (40)$$

where $T_{\gamma_1}(z) = -B_{\gamma_1} G_0(z,\zeta^*)$ and $T_{\gamma_2}(z) = -B_{\gamma_2} G_0(z,\zeta^*)$. We look for $g(z,\zeta^*)$ in a form of the following modified biharmonic single-layer-type potential

$$g(z,\zeta^*) = \int_{\Gamma_0} \left[G_0(z,t) q_1(t) + \frac{\partial G_0(z,t)}{\partial \nu} q_2(t) \right] d_t \Gamma_0, z \in \Omega \quad (41)$$

This potential satisfies the boundary conditions of eqn (39) because of the defining properties of $G_0(z,\zeta^*)$. To determine the densities $q_1(t)$ and $q_2(t)$, the boundary conditions of eqn (40) can be employed. This yields the system of eqn (36) for $q_1(t)$ and $q_2(t)$, where, in this case,

$$K_{11}(z,t) = B_{\gamma_1} G_0(z,t), \quad K_{12}(z,t) = \frac{\partial}{\partial \nu} B_{\gamma_1} G_0(z,t),$$

$$K_{21}(z,t) = B_{\gamma_2} G_0(z,t), \quad K_{12}(z,t) = \frac{\partial}{\partial \nu} B_{\gamma_2} G_0(z,t),$$

and

$$f_1(z) = T_{\gamma_1}(z), \qquad f_2(z) = T_{\gamma_2}(z),$$

Once the solution of the system in eqn (36) is found, values of $G(z,\zeta^*)$ (which represent the plate's deflection due to the transverse unit force concentrated at ζ^*) along with values of its derivatives, required for obtaining stress components, can be readily computed at any point $z \in \Omega$. In Table 6, one finds the values of $G(z,\zeta^*)$ computed by the MMP for the plate whose middle plane occupies the ring-shaped region $\Omega = \{(r,\varphi): .4 \le r \le 1.0, 0 \le \varphi < 2\pi\}$. The inner contour ($r = .4$) is clamped while the outer contour ($r = 1.0$) is simply supported. The point force was applied at $\zeta^* = (.75, .0)$. The Green's function for the circular simply supported plate (see eqn (7)) has been used as $G_0(z,\zeta)$ in the potential of eqn (41).

The computed data have been obtained on two sets of field points. The points of the first set are uniformly spaced on the radius $\varphi = 0$ from the inner contour ($r = .4$) of the ring through its outer contour ($r = 1.0$) (the left fragment of the Table). The points of the second set are uniformly spaced on the circle $r = 0.75$ from $\varphi = 0$ through $\varphi = \pi/3$ (the right fragment). The system in eqn (36) was solved by the trapezoidal rule. The circle of radius .2 centered at the origin has been chosen in this case as the fictitious contour Λ_0.

Table 6 : Deflection $G(z,\zeta^*)$ of the ring-shaped plate under the point force

Point	k		
r	10	20	50
.4	.000000	.000000	.000000
.5	.000813	.000828	.000829
.6	.002372	.002398	.002399
.7	.003744	.003771	.003772
.8	.003668	.003689	.003689
.9	.002066	.002077	.002078
1.0	.000000	.000000	.000000

Point	k		
φ	10	20	50
0.0	.004017	.004042	.004042
$\pi/18$	.003049	.003067	.003067
$\pi/9$	.001854	.001860	.001861
$\pi/6$	.000992	.000996	.000996
$2\pi/9$	.000466	.000479	.000479
$5\pi/18$	.000183	.000206	.000206
$\pi/3$	.000060	.000075	.000076

Since the exact expression for the influence function under consideration is not known, there is no way to rigorously analyze the computed data from Table 6 and to estimate the accuracy level attained. On the other hand, however, the data reveal high convergence rate of the MMP algorithm used in this case (indeed, the data in the columns of $k = 20$ and $k = 50$ differ by only the last of the exhibited decimal place). Hence, given the fact that the potential in eqn (41) represents a biharmonic function which exactly satisfies the boundary conditions on the outer contour Λ, the indicated convergence indirectly confirms the authenticity of the computed data.

References

Brebbia, C.A. (1978): *The Boundary Element Method for Engineers*, Pentech Press, London; Halstead Press, New York

Gradstein, I.S.; Ryzhik, I.M. (1980): *Tables of Integrals, Series, and Products,* Academic Press, New York

Kupradze, V.D. (1965): *Potential Method in the Theory of Elasticity*, Davey, New York

Lebedev, N.N.; Skal'skaya, I.P.; Uflyand, Ya.S. (1966): *Problems of Mathematical Physics,* Pergamon Press, New York

Lovitt, W.V. (1950): *Linear Integral Equations*, Dover, New York

Melnikov, Yu.A. (1977): Some applications of the Green's function method in mechanics, *Int. J. Solids and Structures,* vol. *13,* pp.*1045-1058*

Melnikov, Yu.A. (1982): A basis for computation of thermo-mechanical fields in elements of constructions of complex configuration, *Thesis Dr. Technical Sciences,* Moscow Institute of Civil Engineering (in Russian)

Melnikov, Yu.A. (1995): *Green's functions in Applied Mechanics,* Computational Mechanics Publications, Boston-Southampton

Melnikov, Yu.A. (1999): *Influence Functions and Matrices,* Marcel Dekker, New York-Basel

Smirnov, V.I. (1964): *A Course of Higher Mathematics,* vol. 2 and 4, Pergamon Press, Oxford-New York

Tikhonov, A.N.; Samarskii, A.A. (1963): *Equations of Mathematical Physics,* Macmillan, New York

Timoshenko, S.; Woinowsky-Krieger, S. (1959): *Theory of Plates and Shells,* 2nd ed., McGraw-Hill, New York